

QbD Based Formulation, Optimization and Characterization of Diosgenin and Psoralen Nanoemulgel for Psoriasis

Sandhya Sharma¹, Nayyar Parvez^{1*}, Amarjeet Singh²

¹Research Scholar, School of Pharmacy, Sharda University, Greater Noida, Uttar Pradesh

^{1*}School of Pharmacy, Sharda University, Greater Noida, Uttar Pradesh

²Innovative college of Pharmacy, Greater Noida, Uttar Pradesh

ABSTRACT

Psoriasis is a chronic inflammatory skin disorder which causes excessive proliferation and abnormal differentiation of keratinocytes. Traditional remedies often exhibit constraints, including systemic adverse effects, inadequate skin absorption, and diminished patient adherence. This work intended to create an innovative nanoemulgel system co-loaded with Diosgenin and Psoralen, two phytoconstituents with established anti-psoriatic efficacy, using a Quality by Design (QbD) methodology to solve these obstacles. This work investigates a nanoformulation method for creating a Diosgenin and Psoralen nanoemulsion gel (NEG-2) to boost solubility and improve absorption. The chosen excipients, surfactant/co-surfactant, and oil for the o/w nanoemulsion (NE-G) are Tween 80/Transcutol-P and olive oil. The formulation process employs high-energy ultrasonication with a three-dimensional factorial Box-Behnken design for systematic optimization. The generated nanoemulsion has a 50 nm spherical, globule-like shape, according to the evaluation of its surface morphology using fluorescence microscopy and scanning/transmission electron microscopy. The optimized NE-G exhibited a zeta potential of -25.23 ± 0.18 mV, a size of 195.5 ± 2.65 nm, a polydispersity index (PDI) of 0.37 ± 0.021 , and a pH of 5.9 ± 0.34 . The improved NE-G was then synthesized into a gel with 1% Carbopol 971®. The in vitro release investigation of the improved NEG-2 demonstrated a diffusion-dominant drug release, as per the Higuchi model, during a 24-hour period. The modified nanoemulgel exhibited improved skin penetration, regulated release, and a significant decrease in psoriatic symptoms, validating its potential as an efficacious topical treatment. This QbD-guided methodology guaranteed repeatability, scalability, and robustness of the formulation, creating a potential platform for the administration of herbal actives in the therapy of psoriasis.

Keywords: Psoriasis, Diosgenin, Psoralen, Nanoemulgel, Quality by Design (QbD), Topical delivery, Good health and well-being.

How to cite this article: Sharma S, Parvez N, Singh A. QbD Based Formulation, Optimization and Characterization of Diosgenin and Psoralen Nanoemulgel for Psoriasis. *Int J Drug Deliv Technol.* 2026;16(51s): 1077-1094. DOI: 10.25258/ijddt.16.51s.90

*Corresponding Author: Dr. Nayyar Parvez *Email ID: nparvez2013@gmail.com*

INTRODUCTION

Psoriasis is a long-term inflammatory skin condition that is caused by the immune system and is marked by too many keratinocytes growing, not enough differentiation, and immune cells getting into the skin. It affects around 2–3% of the world's population and makes life much worse because of symptoms including redness, scaling, itching, and thicker plaques. Psoriasis is a complicated disease with several causes[1]. These include genetic factors, environmental triggers, and problems with the immune system, especially with T-helper 17 (Th17) cells and cytokines including IL-17, IL-23, and TNF- α . There are several therapy alternatives available, including as corticosteroids, vitamin D analogues, immunosuppressants, and biologics[2]. However, long-term management is still difficult because of side effects, medication resistance, and patients not following their treatment plans[3]. Topical treatments are still the best way to treat mild to moderate psoriasis since they just work on the area where the psoriasis is and don't do as much harm to the rest of the body[4]. But traditional

topical formulations frequently don't penetrate the skin well, have unstable active components, and don't work very well as medicines. So, we need to quickly come up with new, safe, and effective topical drug delivery technologies that can improve the distribution and effectiveness of anti-psoriatic medicines[5].

Diosgenin and Psoralen are two phytoconstituents that have gotten a lot of interest for their possible use in treating psoriasis symptoms. Diosgenin is a steroidal sapogenin that comes from fenugreek and other plants. It has anti-inflammatory, antioxidant, and antiproliferative effects, which makes it a good choice for treating psoriasis[6]. Psoralen is a furanocoumarin that comes from the plant *Psoralea corylifolia*[7]. It has been used in psoralen treatment for a long time since it may cause apoptosis in hyperproliferative keratinocytes and change how the immune system works. However, the use of these molecules as medicines is restricted by how poorly they dissolve, how easily they pass through the skin, and how stable they are. To get around these problems, nanoemulgels have become potential carriers for delivering

drugs to the skin[8]. Nanoemulgels have the best of both worlds they have the benefits of nanoemulsions (better solubility and permeability) and the benefits of hydrogels (longer retention and easier application). They can efficiently get lipophilic medicines like Diosgenin and Psoralen through the stratum corneum and into deeper layers of skin. They also provide regulated release and better bioavailability[9].

Quality by Design (QbD) method, this study's goal is to create and improve a nanoemulgel formulation that contains both Diosgenin and Psoralen. QbD is a methodical, science-based approach that stresses understanding both the product and the process. Using QbD principles and statistical techniques like Design of Experiments (DoE), it is possible to find, optimize, and control the most important formulation factors to make sure that the product is always the same and works well[10]. The study looks at the formulation development, physicochemical characterisation, in vitro drug release and in vivo anti-psoriatic assessment of the nanoemulgel. The project aims to create a new, strong, and patient-friendly topical delivery method for successful psoriasis therapy employing plant-based actives using this integrated strategy[11].

MATERIALS AND METHODS

Diosgenin and Psoralen were procured from yucca enterprises, Mumbai. The exgratia samples of Transcutol P, Labrasol, Plural, and Capryol 90 were supplied by Gattefosse India Pvt. Ltd. Additional samples of polyethylene glycol, PEG 200, Tween 80, and Tween 20 were procured from Sisco Research Laboratories Pvt. Ltd. (SRL, Mumbai, India). Carbopol 971® was provided by SD Fine Chemicals India Pvt. Ltd. (Mumbai, India). Merck Pvt. Ltd., Mumbai, supplied HPLC-grade acetonitrile and methanol. Loba Chemie Pvt. Ltd. (Mumbai, India) supplied the HPLC water and triethanolamine. CDH supplied lavender oil, kalonji oil, sunflower oil, castor oil, and olive oil from Delhi, India. All additional chemicals, solvents, and reagents used were of analytical grade.

Screening of Excipients

The creation of formulations and the control of stability in a nanoemulsion depend significantly on the effective screening of diverse excipients, including oils, surfactants, and co-surfactants. Accordingly, a variety of oils, including sunflower oil, kalonji, castor, olive, lavender, and Capryol 90 (liquid lipid), were investigated for the current formulation based on the drug's miscibility and solubility. Transcutol P, Tween 80, Tween 20, PEG-200, and Labrasol, were the surfactants and co-surfactants that were taken into consideration for screening based on their individual ionic properties and HLB values. The modified process required the incorporation of an excess quantity of Diosgenin and Psoralen (drug) combined with 1 mL of excipients (oil or surfactant) into a tube, then vortexed (Remi CM-101 cyclomixer; 72 h; 25 °C). The supernatant was collected using a Remi R8C Laboratory centrifuge

after an excess of the medication was allowed to settle after spinning at 3000 ± 50 rpm for 10 minutes. The supernatant was filtered through a $0.22 \mu\text{m}$ syringe filter and vortexed before being diluted with methanol. The quantity of solubilized medication was then quantified by exposing the diluted samples to a UV spectrophotometer set at $\lambda_{\text{max}} 254 \text{ nm}$ [12].

Formulation Development

Preparation of a placebo nanoemulsion

The aqueous microtitration method was utilized to create the placebo NE, after then we assessed the pre-selected oils in conjunction with the surfactant-co-surfactant mixture (Smix), using a Remi cyclomixer (vortex). The chosen oil and Smix were combined and vortexed to create a transparent mixture, then diluted with double-distilled water. The aim of this phase was to assess the compatibility and miscibility of the oils with the Smix and to optimize the Smix quantity using different ratios (1:1, 1:3, 1:4, 2:1, 3:1, 4:1), hence facilitating the creation of a clear NE (Placebo) regarding its visual clarity and turbidity after each dilution. Additionally, in order to create an even greater NE area and draw a pseudo-ternary phase diagram, the oil and Smix ratio was also changed, going from 1:9 to 1:7 to 1:6, 1:5, 1:3.5, 1:2, 2:8, 3:7, 4:6, 5:5, 6:4, 7:3, 8:2, and 9:1 [13].

Preparation of NE

The aforementioned NE was synthesized via a high-energy ultrasonication technique. The requisite quantities of Psoralen and Diosgenin were dissolved in a chosen oil, then solubilized in a Smix. Subsequently, the resultant mixture was microtitrated with double-distilled water to create a coarse pre-emulsion. The pre-emulsion was further processed using an ultrasonic processor UP50H® (Hielscher-Ultrasound Technology, Teltow, Germany) at a frequency of 30 kHz and an amplitude of 40% for 10 seconds to produce a nanosized formulation. The ultrasonication procedure induces cavitation, leading to a temperature rise, which is mitigated by placing the sample container inside an ice-filled beaker [14].

Optimization of Prepared NE: DoE

The Design of Experiments (DoE) software (version 12.0.4, Stat-Ease, Minneapolis, MN, USA) was used to optimize the batches of NE according to predetermined independent and dependent variables. The current formulation incorporates the independent variables and dependent responses of oil concentration (%), Smix ratio (%), sonication duration (s), particle size (nm), polydispersity index, and transmittance (%). The ternary phase diagrams were used to determine the high, medium, and low concentrations of oil and surfactant, as required by the Design of Experiments (DoE). The optimization design used was the Box-Behnken design (BBD), a response surface tool utilized to forecast the impacts of independent factors on dependent responses. Seventeen randomized runs were conducted and analyzed using BBD to get an optimal formulation [16].

Thermal Stability Studies

Thermal stability investigations of the synthesized NE were conducted to assess phase separation, transparency, stability, and droplet size, using the outlined methodology with minor changes [17].

Heating Cooling Cycle

The formulated NE was tested for stability during six cycles at temperatures between 4 and 45 °C. Storage for a minimum of 48 hours at each temperature must be guaranteed.

Centrifugation

The generated NE formulations underwent centrifugation at 4000 rpm for 30 minutes, and those exhibiting no phase separation were chosen for further freeze-thaw processing.

Freeze–Thaw Cycle

For the study to maintain the NE formulations without phase separation (temperature storage for at least 48 hours), freeze-thaw procedures were used after centrifugation at different temperatures between -21 and +25 °C.

Characterization of the Optimized NE**Particle Size, Polydispersity Index (PDI), and Zeta Potential**

The particle size of the optimized NE was assessed using dynamic light scattering (DLS) (Malvern Zetasizer, Nano ZS Worcestershire, UK). The system temperature was kept at 25 °C, the scattering angle was set at 90 °C, and the formulation was diluted at a ratio of 1:50 before and throughout the analysis [18].

Evaluation of entrapment efficacy (EE)

The encapsulation efficiency of the nanocarrier loaded with Psoralen and Diosgenin was assessed using the modified technique outlined. In summary, the produced NE was dried at ambient temperature, after which 5 mg of the dried NE was diluted in 10 ml of HPLC-grade ethanol and then filtered through a 0.22 µm syringe filter. The quantity of Psoralen and Diosgenin NE was quantified spectrophotometrically at 254 nm. The measurement was conducted in triplicate, and the optimal one was chosen for further investigation based on % entrapment. The EE has been calculated using the following equation:

$$\% EE = \frac{W(\text{initial drug}) - W(\text{free drug})}{W(\text{initial drug})} \times 100$$

Where, W(initial drug) is the mass of drug added initially, W(free drug) is the mass of free drug detected in the supernatant after centrifugation[15].

Differential Scanning Calorimetry (DSC)

The DSC analysis of the pure drug Psoralen and Diosgenin and lyophilized sample of the optimized NE formulation was performed using a Pyris 6 DSC, Perkin Elmer, USA. A

brief procedure followed for each sample. A 2 mg sample was taken and subjected to a temperature range of 25–350 °C. The temperature was increased at a rate of 10 °C/min, and the nitrogen flow was maintained at 60 mL/min [19].

Fourier Transform Infrared Spectroscopy (FTIR)

The FTIR analysis of the pure drug Psoralen and Diosgenin and lyophilized sample of the optimized NE formulation was performed using FTIR spectroscopy. First, a precisely weighed quantity of the aforementioned samples (5 mg) was combined with potassium bromide (KBr) in a ratio of (1:1) (different pellets were used for each sample) and then compressed using a hydraulic press to form a flat pellet. The obtained pellets were then scanned between an infrared spectrum of light with a wavenumber of 4500–500 cm⁻¹ [20].

X-ray Diffraction (XRD)

The X-ray diffraction of the pure Psoralen and Diosgenin and lyophilized sample of the optimized NE formulation was performed using an X-ray diffractometer (Philips X-ray generator Poznan, Holland) at a 35 kV electric potential, 30 mA voltage, and detector angle of 2θ (10–70 degree) [17].

Surface Morphology Studies of an Optimized NE**Transmission Electron Microscopy (TEM)**

The optimized NE formulation was examined by TEM (Philips Briarcliff Manor, Briarcliff Manor USA). For the sample preparation, copper grids were inserted into a dust-free paraffin film with forceps, and a drop of the sample (pre-diluted, 1:100) was placed in it using a micropipette. In the same paraffin sheet, 2% of phosphotungstic acid (contrasting agent) was also placed and immersed in the copper grid. A couple of minutes later, the copper grids were removed, dried using a Whatman filter paper, and subjected to TEM analysis [21,22].

Preparation of a Drug-Loaded Nanoemulgel Using an Optimized NE

The optimized NE formulation was prepared as an emulgel with varying proportions of the gelling ingredient, Carbopol 971 0.5% to 1% (w/v). The preparation steps followed a dispersion of Carbopol 971® in distilled water, with continuous stirring. The resultant formulation was sonicated for 15 min to eliminate any air bubbles, followed by the addition of sodium benzoate (a preservative) to obtain a homogenous nanoemulgel dispersion (NEG) [23].

Physicochemical Characterization of NE Gel**Spreadability**

A 0.5 g NE Gel sample was placed on a glass plate pre-marked with a circle of 1 cm in diameter, and another glass plate loaded with a 500 g weight was placed above it for 5 min. An increase in the diameter of a gel surface can indicate its spreadability using the following formula:

$$W \cdot L / t = S$$

where:

S—spreadability (g/s)
 W—weight on the glass plate (g)
 L—length travelled by the glass plate
 t—time taken (s)

The test was performed in triplicate, and a linear scale was used to determine the extension required to separate the glass plates [24].

Extrudability

The measurement of extrudability determines the ease of expulsion of a formulation from a tube, i.e., 0.5 cm of the formulation in 10 s. The crimped end of a closed collapsible tube with a pre-weighed amount of the optimized NEG was taken, and a firm pressure was applied. After a certain length of time, the pressure was released, and the tube cap was removed to note the amount of extruded gel using a linear scale. The higher the extruded quantity is, the higher the extrudability will be [25].

Texture Analyzer

A glass jar containing the NEG sample was placed on a flat testing surface to avoid premature triggers and air bubbles. The texture profile assessment of the firmness, cohesiveness, consistency, and viscosity indices was conducted in a compression mode using a texture analyzer (TA. Plus, Stable Micro Systems, Surrey, UK). The results were noted as force–time graphs to determine several mechanical characteristics of the NEG [19].

In-Vitro Drug Release Study

The release profile of the pure drug, NE, and NEG-2 formulations (containing a 5 mg equivalent of Psoralen and Diosgenin) was performed through a pre-activated dialysis bag (m.wt. 12,000 Dalton). The test media used was phosphate saline buffer (pH 5.8) (250 mL) at 600 rpm and temperatures of 37 ± 0.5 °C. Then, 2 mL samples were collected at pre-determined time intervals and immediately replaced with an equal amount of dissolution

media to balance the sink conditions. The aliquot collected was then filtered, diluted, and analyzed using a pre-validated UV spectroscopy method at wavelength of 254 nm [26].

Storage Stability of the Optimized Nanoemulsion

The stability investigation of the optimized NE was conducted at room temperature (25 °C \pm 1 °C) for 15 weeks. Two drug formulations were evaluated for their stability to determine whether sonication affects the long-term storage. One consisted of an optimized NE without sonication, and the other was an ultrasonically customized NE. The size distribution was the parameter chosen for the stability studies. After completing 0, 1, 3, 7, 10, 13, and 15 months of storage, variations in the nanoemulsion droplet size were investigated [27–31].

RESULT AND DISCUSSION

Formulation of Nanoemulsion

Screening of Excipients

The solubility of Psoralen and Diosgenin in various excipients was investigated, and the findings are presented in Figure 1. Amongst the different experimental oils, the highest solubility (120.18 ± 0.60 mg/mL and 158.85 ± 0.21 mg/ml) of Psoralen was observed in the castor oil, making it a suitable oil phase for the purported formulation. Tween 80 and Transcutol-P were selected as the surfactant and co-surfactant, respectively, as they showed the maximum drug solubility, i.e., 63.23 ± 0.157 mg/mL and 150.32 ± 0.63 mg, respectively, as well as miscibility (Table 1). Furthermore, the combination (Smix ratio) of Tween 80 and Transcutol-P was selected via employing pseudo-ternary phase diagrams to produce a clear NE using the placebo formulations. Drug solubilization studies are critical for NE development, as they play a crucial role in the formulation stability, delivery, and maintenance. The selection of suitable excipients is also necessary to produce a transparent, clear, homogenous formulation with a high binding capacity for API (amongst other reasons).

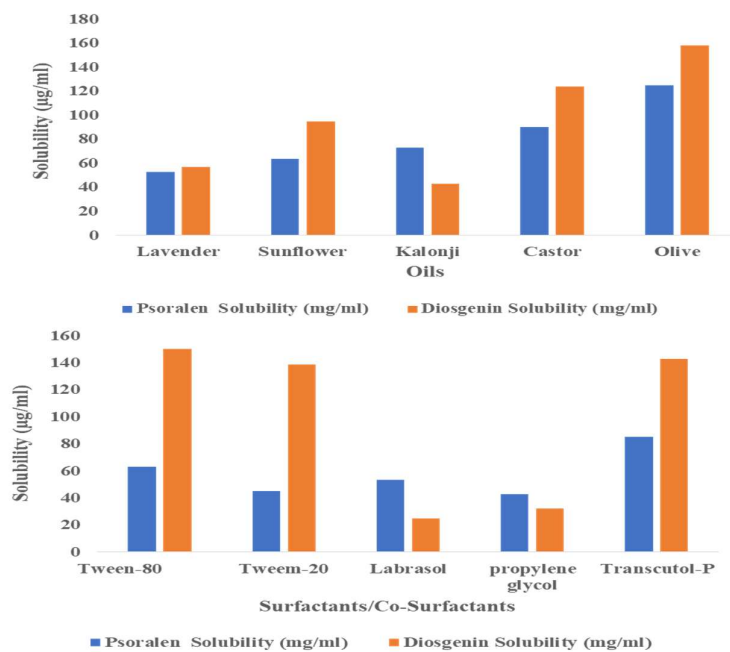


Figure 1:Psoralen and Diosgenin solubility in various surfactants, co-surfactants, and oils.

Table 1:Screening of Oils, Surfactants, and Co-Surfactants based on miscibility.

S. No	Oils	Surfactants	Co-Surfactants	Inference
1	Lavender	Tween-80	Transcutol-P	No Phase separation
2	Sunflower	Tween-80	Transcutol-P	Phase separation
3	Kalonji	Tween-80	Transcutol-P	Phase separation
4	Castor	Tween-80	Transcutol-P	No phase separation
5	Olive	Tween-80	Transcutol-P	No Phase separation
6	Sunflower	Labrador	Transcutol-P	No phase separation
7	Kalonji	Labrador	Transcutol-P	Phase separation
8	Lavender	Labrador	Transcutol-P	No phase separation
9	Castor	Labrador	Transcutol-P	Phase separation
10	Olive	Labrador	Transcutol-P	Phase separation

Formulation development

Preparation of a placebo nanoemulsion and excipients optimization

The combination of the selected surfactants was further evaluated for the Smix ratio using a pseudo-ternary phase diagram Figure 2, in which a dotted color represents an NE region. As observed, the Smix ratio of 1:4 produced the lowest nanoemulsion zone, whereas a Smix ratio of 2:1 produced the highest nanoemulsion zone. This could be due to a high HLB of Tween-80 and the fact that, subsequently, when the Tween 80 concentration is increased, the HLB of the Smix also increases. However, this explanation does not comply with a Smix ratio of 3:1, in which an increase in the Tween 80 concentration enhances the viscosity simultaneously, leading to droplet disruption and breakage in the NE [32]. The selected Smix

ratio was then used to produce various placebo formulations, as the pseudo-ternary phase diagrams were also helpful in identifying the minimum and maximum proportions of oil and Smix to be used to obtain a clear, transparent, and homogenous NE. Notably, of the many combinations tested for an *o/w* NE preparation, only two were taken for further analysis, in which the minimum ranges of the oil phase and Smix were 1–2.5% and 16–18%, respectively. Below a concentration of 1%, the oil phase was incapable of solubilizing the required amount of API. At a concentration higher than 2.5%, it exceeded the percentage of water, leading to a formation of *w/o* NE. Additionally, a higher percentage of the oil phase requires a much higher concentration of Smix, i.e., more than 20%, leading to microemulsion rather than a purported NE [23].

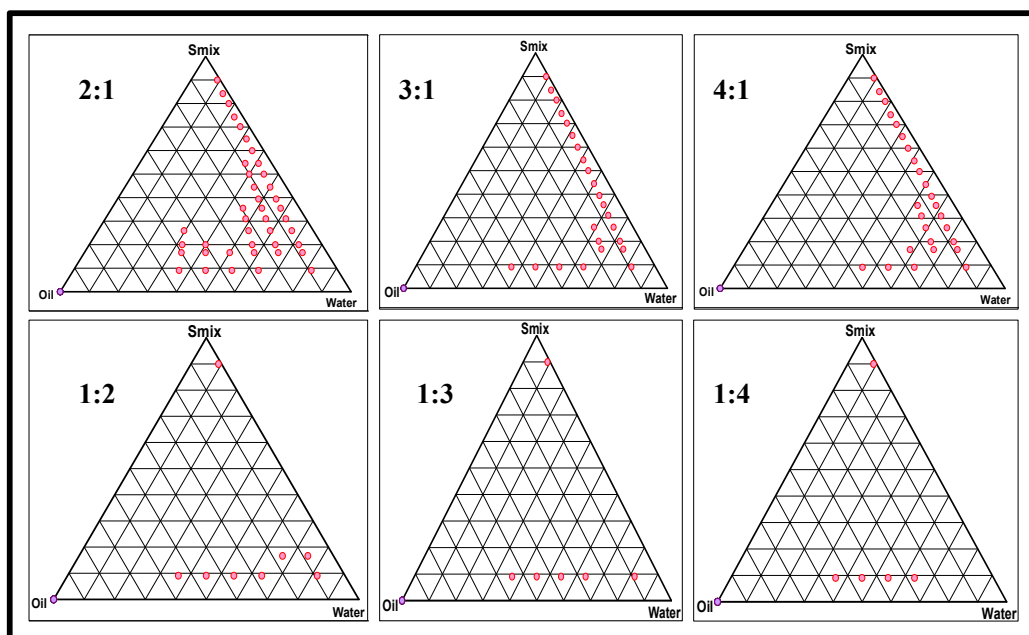


Figure 2: Pseudo-ternary phase diagrams for various Smix ratios

Preparation of a drug-loaded NE

After carefully selecting various excipients and their optimized concentrations, a methodology suitable for the preparation of a NE was adopted. The ultrasonication technique is a highly popular process employed for NE fabrication. It has the upper hand over the high-pressure homogenization technique due to the promised integrity of the NE droplets in terms of their shape and dispersion. In an HPH (high-pressure homogenizer), the size of a droplet may be smaller, but the surface can be irregular due to the high process. Additionally, the NE formed may have a high PDI, leading to polydisperse formulation [33-34]. Furthermore, an increase in temperature during the processing may adversely impact the formulation outcomes. Additionally, the high cost and maintenance may limit its commercial potential [35]. Henceforth, ultrasonication was selected as the method of choice for the fabrication of the Psoralen and Diosgenin NE.

BBD: mathematical model fitting and optimization of Psoralen and Diosgenin NE

For the present formulation, the independent variables and dependent responses selected were the oil concentration (%), Smix ratio (%), starting time (s) and particle size (nm), polydispersity index (PDI), and Entrapment Efficacy (EE) (%), respectively. The ternary phase diagrams were utilized to select the high, medium, and low levels of the oil and surfactant concentrations required for DoE. The optimization design followed was the BBD, a response surface methodology approach used to predict the effects of independent variables on dependent responses (Table 2). The varied levels or experimental ranges for the selected independent variables are presented in (Table 3). As observed, all three dependent responses followed a polynomial quadratic model, with a non-significant lack of fit ($p > 0.05$) (Table 4). The observations of the BBD were recorded as 3D response surface graphs (Figure 4) for a comparative illustration of the interaction of each dependent response with two different independent variables [36]. Following are the detailed descriptions of each response:

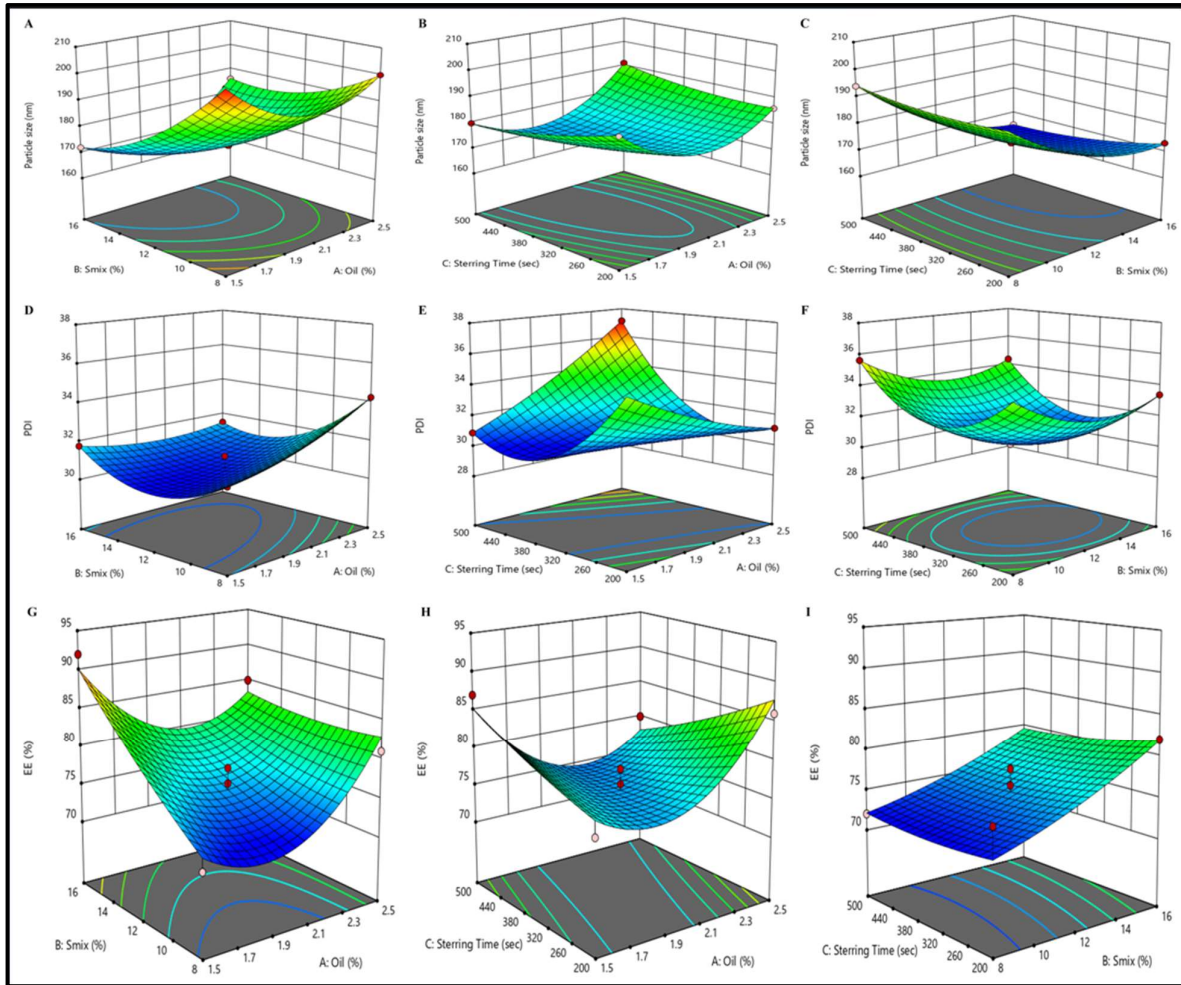


Figure 4:3D response surface depicting the interaction effect of the independent variables like oil, smix, Stiring time on (A-C) particle size, (D-F) PDI, and (G-I) % EE.

Table 2: BBD-based NE with independent and dependent variables.

Run	Oil (%)	Smix (%)	Stiring Time (Sec)	Particle size (nm)	PDI	EE (%)
1	2	8	500	194	0.35	72
2	2	12	350	173	0.30	74
3	2.5	16	350	186	0.31	85
4	2.5	12	200	186	0.31	86
5	1.5	12	200	190.77	0.34	76
6	2.5	12	500	191.23	0.37	80
7	2	12	350	173	0.30	76
8	2	12	350	173	0.30	75
9	2	16	500	164.89	0.34	76
10	2	12	350	173	0.30	73
11	1.5	8	350	208	0.31	72
12	1.5	16	350	172.03	0.31	92
13	2	12	350	173	0.31	78
14	2	16	200	173.2	0.33	82
15	2	8	200	193	0.34	76
16	1.5	12	500	179.83	0.30	87
17	2.5	8	350	200	0.34	81

Table 3: Selected independent variables and their levels.

Independent variables	Levels		
	Low	Medium	High
X1 = Oil (%)	1.5	2	2.5
X2 = Smix (%)	8	12	16
X3 = Stirring time (sec)	350	200	500

Table 4: Regression analysis summary for responses Y1 (Particle size in nm), Y2 (PDI), and Y3 (%EE)

Quadratic model	%CV	R ²	Adjusted R ²	Predicted R ²	SD
Particle size (Y1)	0.14	0.9998	0.9995	0.9965	0.27
PDI (Y2)	1.04	0.9898	0.9768	0.9841	0.33
% EE (Y3)	3.94	0.8758	0.7161	0.5947	3.11
<p>Y1 = Particle size +173.00+1.58*A-12.36*B-1.63*C+5.49*AB+4.04*AC-2.33*BC+12.10* A²+6.41* B²+1.86* C²..... Equation (1)</p> <p>Y2 = PDI +30.40+0.6250*A-0.6250*B+0.5000*C-0.7500*AB+2.50*AC+0.0000*BC+ 0.4250* A²+1.43* B²+2.68* C².....Equation (2)</p> <p>Y3 = Stirring time +75.20+0.6250*A+4.25*B-0.6250*C-4.00*AB-4.25*AC-0.5000* BC+6.53* A²+0.7750* B²- 0.5250 *C²..... Equation (3).</p>					

Effect of independent variables on particle size

Its nature is one of the distinct features of NE. The smaller the size is, the larger the surface area which ultimately affects the drug delivery, permeation, and bioavailability will be. However, the particle size might vary due to the effects of variables, as discussed further below. For example, with an increase in the oil concentration, the particle size increases due to the increased chain length (Figure 4), and as the present formulation is *o/w* NE, a larger oil droplet size may contribute to a large particle size as well [37]. It was also observed that the Smix ratio and sonication time do not affect the particle size (Figure 3 A–C). As presented in Table 2 all 17 formulations had a particle size range of 173 ± 0.21nm.

Effect of independent variables on PDI

A PDI represents the formulation consistency in terms of the particle dispersion, i.e., monodisperse or polydisperse. Such a dispersion of the formulation particles might indicate their uniformity and degree of aggregation and may affect the drug distribution [38]. As shown in the BBD graphs, all three independent variables had considerable effects on the PDI (Figure 3 D–F). Furthermore, all 17 formulations had PDI values in the range of 0.30 ± 0.016 (Table 2), which was sufficiently suitable, as a high PDI of more than 0.3 generally signifies particle agglomeration, which may increase the particle size [39].

Effect of independent variables on %EE

The %EE value reflects the amount of incident light that passes through a formulation or sample without being changed, i.e., it is neither absorbed nor scattered. Notably, the %EE values for clear solutions/dispersions are higher. In contrast, those for cloudier/turbid solutions/dense dispersions are lower, as more incident light can be transmitted through a clear sample rather than a turbid one. For an NE, the more refined/fine the particles are, the greater the transmittance will be. For the present formulation, each independent variable had a distinct impact on the %EE (Figure 3 G–I), and the predicted 17 formulations elicited values range from 75.2 ± 0.42%. Conclusively, the obtained range is suitable (transparency and clarity) and complies with the other dependent responses as well [40]. After evaluating each variable, the formulation, with a particle size of 173 ± 0.21nm, PDI of 0.30 ± 0.016, and %EE of 75.2 ± 0.42%, was selected as the optimum formulation.

Thermodynamic stability

Thermal stability studies, such as heating–cooling, centrifugation, and the freeze– thaw cycle, revealed that certain NE formulations were turbid, and some had phase separation (Table 5). Such instability might occur due to Ostwald ripening, a free-surface energy process in which small droplets combine via diffusion to form aggregates or larger droplets [41]. The formulations which did not show any thermodynamic instability were subjected to further physical characterization, as highlighted in Table 6. The collated results of both the thermodynamic and physical characterizations revealed the formulation as the most suitable and optimized NE.

Table 5: Thermodynamic stability testing of selected nanoemulsion formulations using heating cooling (HC), freeze-thaw (FT), and Centrifugation (Cent).

Six ratios	Formulation coding	Percentage of component % (v/v)			Observation			Inference
		Oil	Smix	Water	Heating	Freeze-	Centrifugation	

					cooling	thaw		
S Smix = ratio 2:1	S-1	2.22	17.78	80	✓✓	✓✓	✓✓	Passed
	S-2	2	14	85	×	×	×	Passed
	S-3	2.5	17.5	80	✓	×	×	Failed
	S-4	7.74	47.09	45.3	✓	×	×	Failed
P Smix = ratio 3:1	P-1	1.67	13.33	85	×	✓	✓	Failed
	P-2	1.87	13.12	85	×	×	×	Failed
	P-3	2	14	85	✓	✓	✓	Passed
	P-4	2.86	17.14	80	✓	×	×	Failed
G Smix = ratio 4:1	G-1	2.78	22.12	75	✓	✓	✓	Passed
	G-2	3.13	21.78	75	✓	✓	✓	Passed
	G-3	2.5	12.5	85	✓	×	×	Failed
	G-4	2	18	80	×	×	×	Failed

Table 6: Physical characterization studies of various nanoemulsion formulations.

Formulation coding	Particle size (nm) (Mean± SD) (N=3)		PDI (Mean± SD) (N=3)		pH (Mean± SD) (N=3)		RI (Mean± SD) (N=3)		Viscosity (mp) (Mean± SD) (N=3)	
	Blank	NE	Blank	NE	Blank	NE	Blank	NE	Blank	NE
S	150.6 ± 1.34	224.7 ± 1.30	0.24 ± 0.05	0.28 ± 0.03	5.9 ± 0.34	6.1 ± 0.44	1.401 ± 0.006	1.402 ± 0.008	43.31 ± 3.24	43.78 ± 2.42
P	41.13 ± 1.45	72.34 ± 1.43	0.16 ± 0.02	0.13 ± 0.03	5.8 ± 0.25	5.8 ± 0.32	1.405 ± 0.003	1.405 ± 0.007	134.0 ± 6.42	138.5 ± 3.08
G	100.13 ± 1.74	187.6 ± 1.23	0.18 ± 0.04	0.23 ± 0.02	5.6 ± 0.13	5.7 ± 0.25	1.402 ± 0.002	1.368 ± 0.004	104.0 ± 3.40	106.0 ± 3.49

Characterization of an optimized NE-G

Particle size, polydispersity index (PDI), and zeta potential

The optimized, revealed a droplet/particle size of 195.5 ± 2.65 nm (diameter), PDI of 0.37 ± 0.021 (Figure 5), and zeta potential of - 25.23 ± 0.18 mV. As noted earlier, the nano size ensures an adequate surface area and more efficacious drug delivery, absorption, and retention. Generally, the NE-G falls in a diameter range of 5–200 nm, and based on the obtained results of the present NE-G, the

size range was concordant. A low PDI point to the monodisperse nature of a prepared formulation. Additionally, it indicates a high concentration of the surfactant, which forms a densely packed film at the oil–water interface, thus providing a greater stabilization/emulsification of the oil phase, rather than the co-surfactant. The negative value of the zeta potential could be due to the incorporation of non-ionic surfactants, which are expected to stabilize and lower the charge magnitude of the dispersed oil droplets [42].

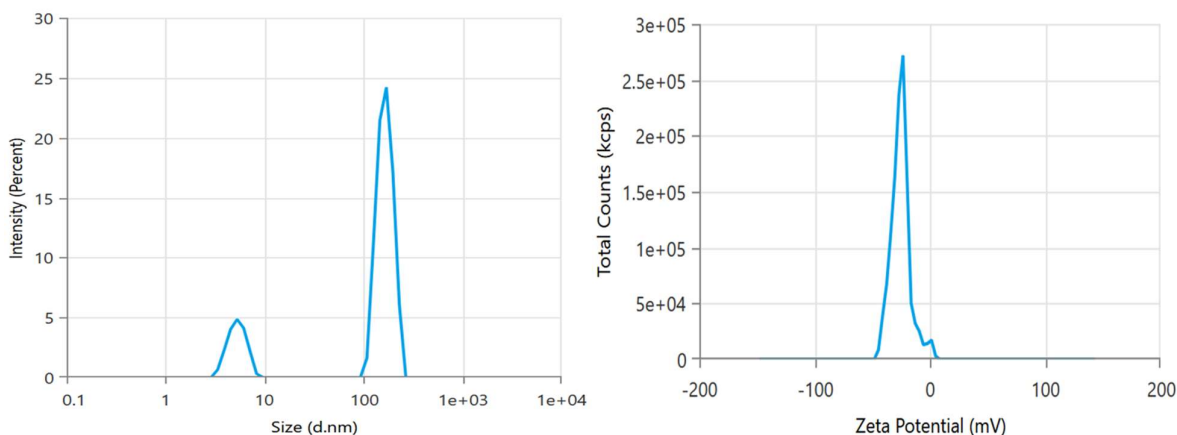


Figure 5: Particle size, polydispersity index (PDI), and zeta potential of NE-G.

Evaluation of EE

Psoralen and Diosgenin NE were characterized by physicochemical and spectroscopic methods. Following the successful synthesis of several nanoparticle batches, the encapsulation efficiency % of Psoralen and Diosgenin NE was assessed. The proportion of EE was assessed spectrophotometrically at 254 nm. The findings indicate that NE-G exhibits the greatest percentage of encapsulation efficiency (EE) for NE-G, at $75.2 \pm 0.42\%$

w/w, respectively. Likewise, a research referenced by Ige et al. indicated a maximum % EE of 70-80% w/w. Consequently, based on the percentage of drug entrapment, NE-G was identified as the optimum nanoemulsion and was subjected to additional investigation, including physicochemical parameters and gel formation. The percentage of drug entrapment for all NE groups is shown in Figure 3.

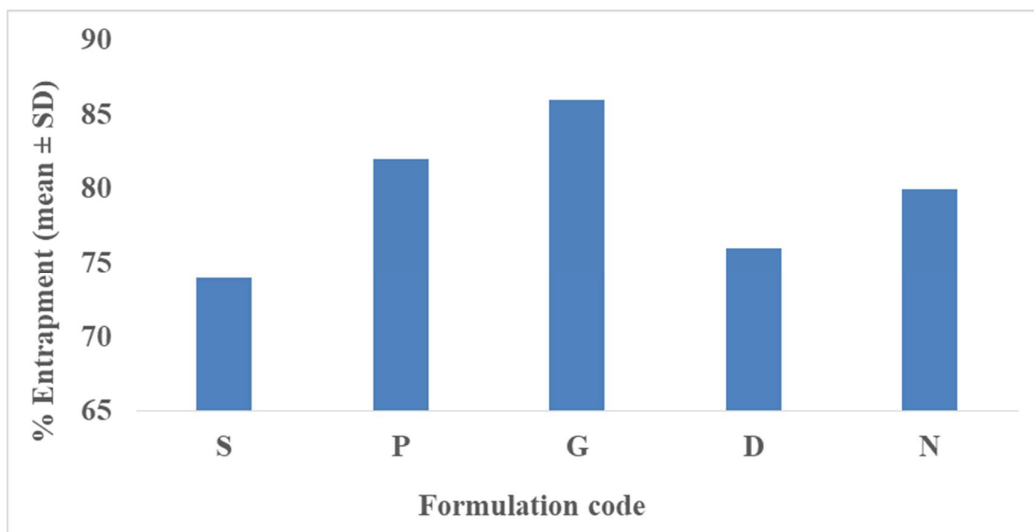


Figure 3: Percentage entrapment efficiency of NE-G

Differential Scanning Calorimetry (DSC)

The melting point of the pure drug was estimated to be 168.87 and 211.27°C (area 567.044 and 81.525mJ) (Figure 6), which corresponds to the reported melting range of 168.87 and 211.27°C. The obtained peak was found to be endothermic, and the nature of the drug was crystalline. However, in the DSC thermogram of the lyophilized NE-G formulation, only a single peak at 169.83 °C was noted

(area 401.586 mJ). The obtained peak was the lyophilization of the optimized NE-G. The single peak could be due to the high quantity of mannitol, while also depicting the transition of the NE-G from a crystalline state. This could further accrue stability in terms of the drugs leaching or precipitation within the proposed formulation.

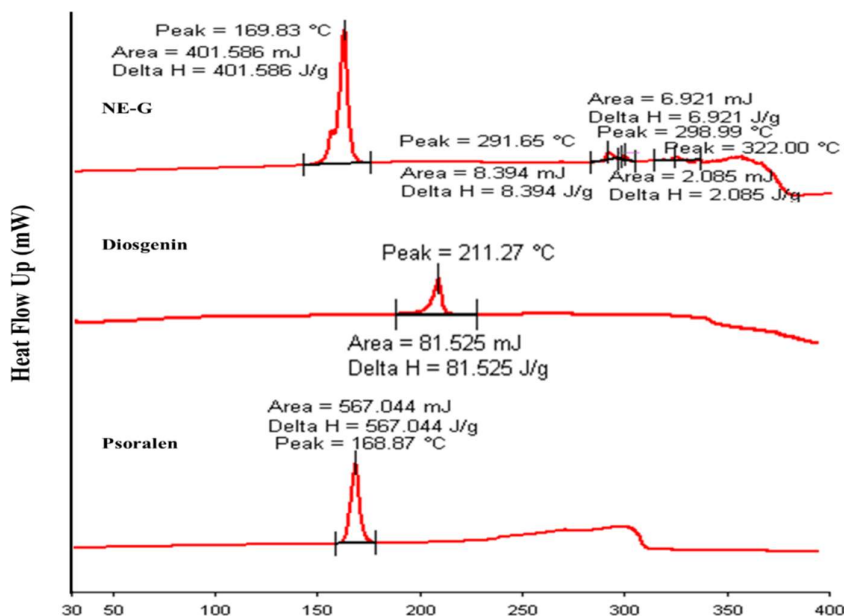


Figure 6: Overlay of Differential Scanning Calorimetry (DSC) Psoralen, Diosgenin, and NE-G

Fourier Transforms Infra-Red Spectroscopy (FTIR)

The FTIR spectra of a NE-G (Figure 7) Psoralen showed characteristic peaks (cm⁻¹) as noted as 3061.52 (C-H Stretch Aromatic vinyl hydrocarbon), 1758.26 (C=O carbonyl Group), 1541.53 (C=C Double Bond), 1448.23, 1261.64, 1184.13, 1021.94 (Ether group C-O-C). Diosgenin spectrum showed bands at 3447.62, cm⁻¹ corresponds to -OH stretching, and the bands at 2949.57 cm⁻¹ and 1456.84 cm⁻¹ corresponding to CH₂ stretching and scissoring vibration, respectively. Strong characteristic peaks at 1171.21 cm⁻¹ and 1052.08 cm⁻¹ can be attributed to -C-O stretching, and the band at 895.63 cm⁻¹. The FTIR spectra of the lyophilized NE-G (KBr), the

bands were observed at spectrum showed bands at 3331.36, cm⁻¹ corresponds to -OH stretching, and the bands at 2971.10 cm⁻¹ corresponding to CH₂ stretching and scissoring vibration, respectively. Strong characteristic peaks at 1158.30, 1132.46, 1102.32, and 1092.27 cm⁻¹ can be attributed to -C-O stretching, and the band 1733.86 cm⁻¹, C=O carbonyl Group Collectively, a slight shift in the peaks was observed in the spectra of the lyophilized NE-G as compared to the Psoralen and Diosgenin, thus indicating its amalgamated/complexed nature [43]. In the case of the mannitol, the peaks were very close to the NE-G spectra, as it was used in excess to ensure an effective lyophilization of the NE-G.

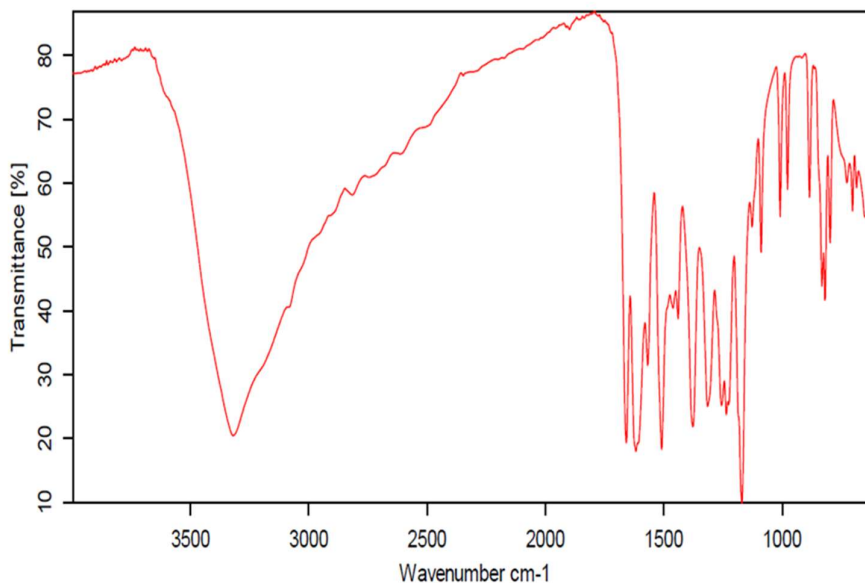


Figure 7: Overlay spectra were showing FTIR of NE-G.

X-Ray Diffraction

As shown in Figure 8, the XRD spectra of the NE-G, revealed a crystalline form with sharp peaks at the 2θ values 16.3° and 15.6° . The lyophilized formulation had no prominent peaks and had to be converted from a crystalline to an amorphous form. A few large peaks can also be seen at the peaks at the 2θ values 5° to 35° . These peaks belong

to the mannitol, which was also included as a cryoprotectant during the lyophilization process, but the peaks were reduced to an amorphous nature in the formulation. As a result, the lyophilized formulation might be described as amorphous, and this conclusion was supported by the DSC patterns, as discussed earlier in this section.

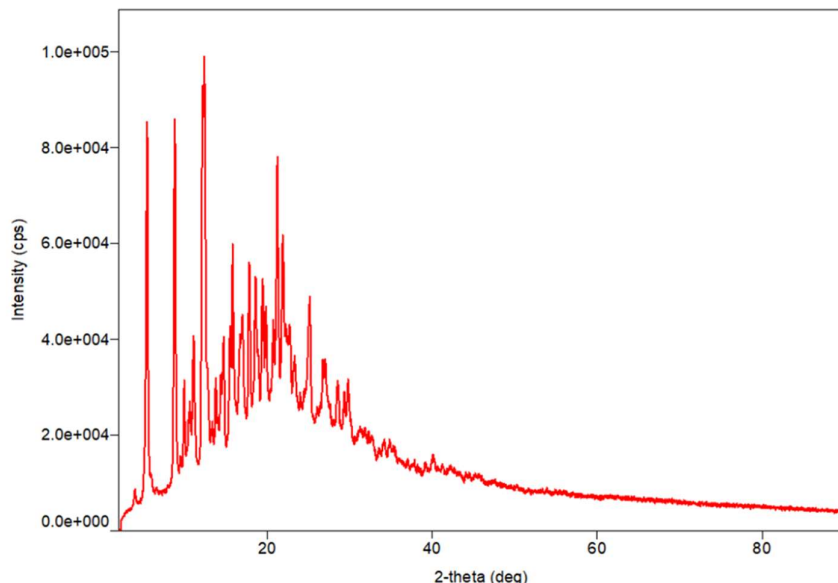


Figure 8: Overlay of X-Ray Diffractograms of NE-G.

Surface morphology

TEM microscopy

The three different techniques were employed to analyze the structure and surface morphology of the final formulation. They collectively revealed a circular, globule-like structure with a size range below 50 nm (Figure 9).

Furthermore, the obtained size range corroborated well with the observations of the zeta sizer. Thus, the optimized formulation is acceptable in terms of its shape and size, i.e., nanometric and globular size, respectively, for an efficient topical delivery permeation and retention.

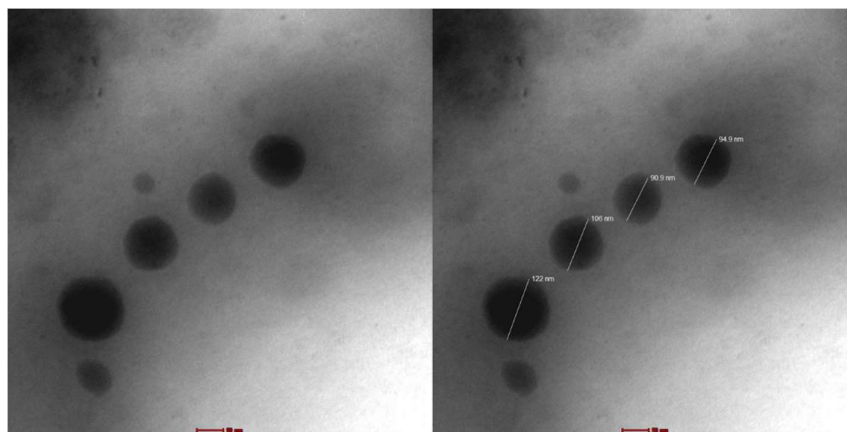


Figure 9: TEM microscopy of optimized NE-G.

Characterization of Nanoemulsion Gel Spreadability and Extrudability

Various placebo gel preparations with different optimized NEG-2 did not have a coarse texture and was

concentrations of Carbopol 971 were evaluated, and the concentration of 1% showed acceptable results. The optimized NEG-2 did not have a coarse texture and was

smooth and homogenous. The pH of the optimized gel was 5.8 ± 0.57 , which could be inferred as safe and non-irritating to the skin. The spreadability and extrudability mainly contribute to an easy application at the desired site and expulsion from the packaging, respectively. Thus, they are critical for a high patient compliance. The optimized NEG-2 has a spreadability of 17.38 ± 1.45 g.cm/s and extrudability of 5.56 ± 1.13 g [44].

Texture analysis of Placebo and formulation

The textural properties, depicted in Figure 10, were

assessed for both the placebo and the optimized formulations. For the optimized NEG-2 gel, cohesiveness was determined to be -27.78 g, showing its capacity to adhere when subjected to tensile stress. Firmness was found to be -41.09 g, indicating its resistance to compressive force and maintaining its structural integrity. Furthermore, consistency was measured at 393.98 g.sec, and the viscosity index was -213.90 g.sec, highlighting the formulation's stability, suitability for packaging, and ease of use [45].

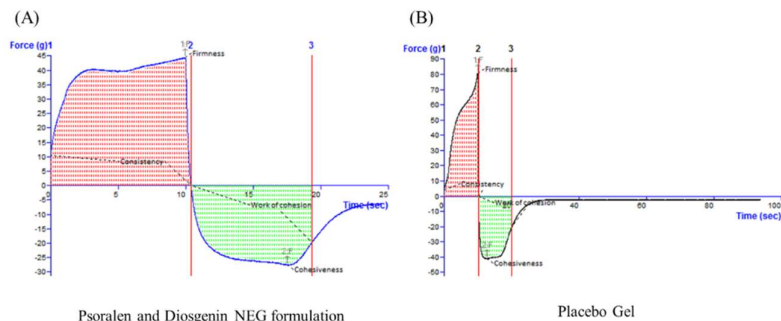


Figure 10: Texture analysis of NEG-2 (A) and Placebo Gel (B).

Drug release/permeation profile

In Vitro Drug Release Study

The cumulative release profiles for each optimized formulation, Placebo Gel and NEG-2 were performed using a dialysis membrane, calculated, and compared graphically, as presented in Figure 11. The % cumulative drug release (%CDR) for the different formulation types was found to be $86.58 \pm 2.14\%$ (NEG-2), $75.27 \pm 2.12\%$ (Placebo Gel) after 24 h. the optimized NEG-2 displayed a biphasic release behaviour with a rapid release pattern in the initial 4 h, followed by a slow release afterwards. The initial fast release could be due to the presence of the drug on the formulation surface, and the following slow release may be due to drug entrapment in the gel matrix, which

may hinder the diffusion. Additionally, the increased viscosity of NEG-2 due to its incorporation into the gel matrix may impede the diffusion process. As mentioned in the literature, NE formulations have various rate-controlling drug release mechanisms, such as diffusion, swelling, and erosion [46]. To pinpoint the mechanism for the present formulation, different release kinetic models were employed, such as zero-order, first-order, and Higuchi models, and the drug release was diffusion-dependent (Korsmeyer Peppas model, $R^2=0.9583$). The Higuchi models encourage the release of low-soluble APIs dispersed in a uniform semi-solid or solid matrix, which behaves as a diffusion medium.

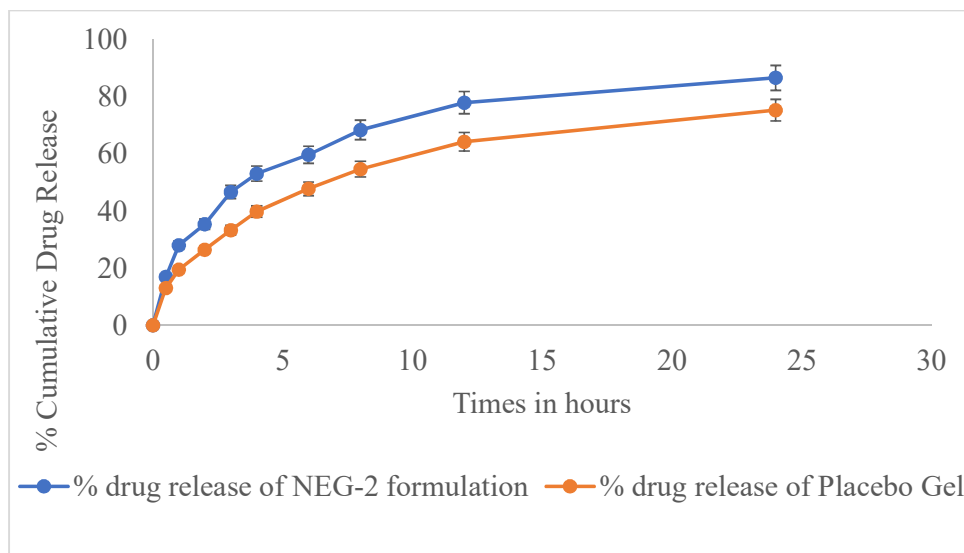


Figure 11: In vitro drug release of NEG-2 and Placebo Gel.

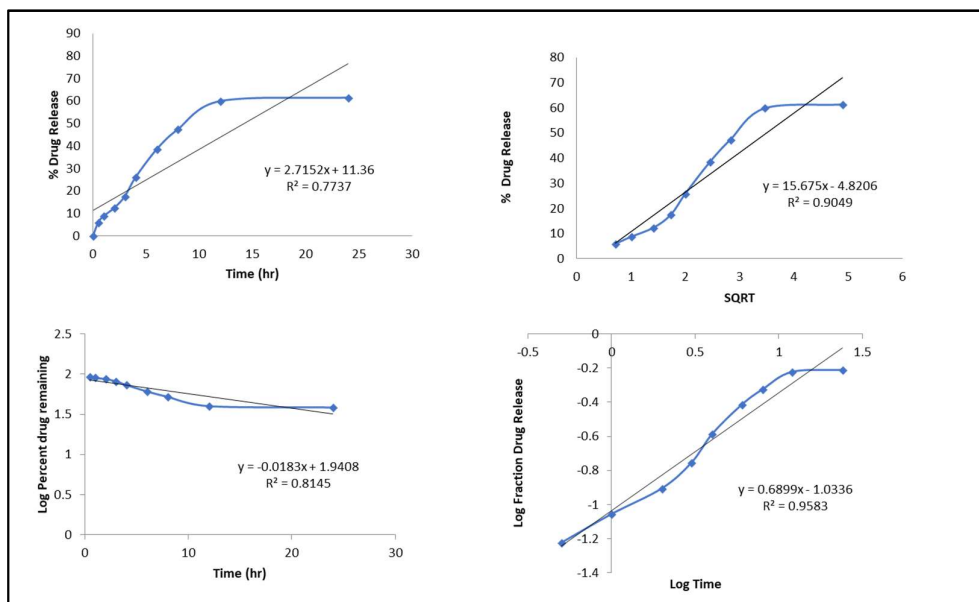


Figure 8: Kinetic model graph of NEG-2 and Placebo Gel.

Table 7: Kinetic models of *in-vitro* release

Zero order		First order		Higuchi		Peppas	
R ²	K ₀	R ²	K ₀	R ²	K ₀	R ²	K ₀
0.7737	2.7152	0.8145	0.0183	0.9049	15.675	0.9583	0.6899

Stability study

The ultrasonication method was used to develop the NEG-2 formulation which was reported to be stable for 12 week (Table 8). In the optimized NEG-2 formulation prepared without ultrasonication, phase separation occurred after only 4 month. The Z-average particle diameter and PDI of NEG-2 formulation at the beginning (0 week) were 74.36 ± 1.41 nm and 0.145 ± 0.016, respectively. The diameter of the droplets expanded rapidly from 0 to 7 week, most likely due to their significant Ostwald ripening rate. In the

first three weeks, the turbulence created accelerated the mobility of the droplets and tightened the connections between them, leading to molecular diffusion and Ostwald ripening. The PDI of the formulation likewise increased, showing a variation in the droplet size uniformity. According to the droplet size measurements, the droplet size increased a little after three and seven weeks, indicating a stable formulation. However, after 10 week, there was another increment in the droplet size but no evidence of phase transition. NEG-2 formulation had an

initial particle size of 124.3 ± 5.16 nm and a PDI of 0.251 ± 0.026 , respectively. The droplet size increased dramatically to 135.3 ± 4.05 nm after one week, and the PDI improved (0.143 ± 0.21). After 10 week, the average droplet size above 150 nm, and phase transition was observed in NEG-2 formulation [47]. Micelle swelling occurs due to this process, and any micelles that are not absorbed remain in the formulation. Micelles disrupt the stability by causing droplet agglomeration. There was a significant difference between the Z-averages of NEG-2 formulation before and after sonication in the stability investigation. This is because their Ostwald ripening

processes varied. In conclusion, the better storage stability observed in NEG-2 formulation is likely due to a lower Ostwald ripening rate [48]. The sluggish Ostwald ripening of NEG-2 formulation could be attributed to the lack of micelles and the initially reduced droplet size. Therefore, the formulation remained stable for 12 week, despite its low zeta potential (-2.65 ± 0.27 mV). Tween-80, a non-ionic surfactant, also aids in the steric stabilization of the nanoemulsion and thus its stability. According to the stability study, a nanoemulsion that is ultrasonic-assisted and QBD-validated enhances the nanoemulsions long-term stability

Table 8: Stability study of optimized NEG-2

Duration (Week)	NEG-2 formulation (Before sonication)		NEG-2 formulation (After Sonication)	
	Particle size (nm) (n=3 \pm SD)	PDI (n=3 \pm SD)	Particle size (nm) (n=3 \pm SD)	PDI (n=3 \pm SD)
0	93.12 ± 3.11	0.329 ± 0.71	74.36 ± 1.41	0.145 ± 0.016
1	141.3 ± 6.01	0.143 ± 0.42	95.03 ± 3.02	0.162 ± 0.075
2	147.2 ± 12.81	0.234 ± 0.012	105.8 ± 5.12	0.182 ± 0.016
4	241.4 ± 14.89	Phase separation	108.2 ± 6.03	0.217 ± 0.043
7	Phase separation	Phase separation	124.3 ± 5.17	0.231 ± 0.036
10	Phase separation	Phase separation	122.5 ± 9.10	0.248 ± 0.024
12	Phase separation	Phase separation	135.8 ± 7.31	0.292 ± 0.013

CONCLUSIONS

The proposed study investigated a Diosgenin and Psoralen-based nanoemulsion gel/nanoemulgel using ultrasonic techniques and "Quality by Design" (QbD) methodologies. The amalgamation of Diosgenin and Psoralen inside a nanoemulgel is a potentially efficacious formulation strategy, leveraging the therapeutic properties of Diosgenin and Psoralen for the intended uses of the topical formulation. The NEG-2 nanoemulgel exhibits superior pharmaco-technical characteristics, including better solubility and improved in-vitro release, as anticipated. The bioavailability of Diosgenin and Psoralen may facilitate their clinical use as alternative therapies for difficult diseases, such as psoriasis. The potential of the improved formulation is anticipated to be greater and merits exploration in preclinical and, ultimately, clinical contexts.

Funding: No external funding.

Conflicts of Interest: The authors declare no conflict of interest

REFERENCES

1. S. Mohammadi nejad, h. Özgüneş, n. Başaran, Pharmacological and Toxicological Properties of Eugenol, Turkish Journal of Pharmaceutical Sciences. (2017). <https://doi.org/10.4274/tjps.62207>.
2. S. Akhter, F.M. Tasnim, M.N. Islam, A. Rauf, S. Mitra, T. Bin Emran, F.A. Alhumaydhi, A. Ahmed Khalil, A.S.M. Aljohani, W. Al Abdulmonem, M. Thiruvengadam, Role of Th17 and IL-17 Cytokines on Inflammatory and Auto-immune Diseases, Current Pharmaceutical Design. (2023). <https://doi.org/10.2174/1381612829666230904150808>.
3. M.R. Haghshenas, M.R. Zamir, M. Sadeghi, M.J. Fattahi, K. Mirshekari, A. Ghaderi, Clinical relevance and therapeutic potential of IL-38 in immune and non-immune-related disorders, European Cytokine Network. (2022). <https://doi.org/10.1684/ecn.2022.0480>.
4. R.J. Chandy, S.G. Bridgeman, B.M. Godinich, S.R. Feldman, New synthetic pharmacotherapeutic approaches to the treatment of moderate-to-severe plaque psoriasis in adults, Expert Opinion on

- Pharmacotherapy. (2023). <https://doi.org/10.1080/14656566.2023.2206014>.
5. K. Yadav, A. Soni, D. Singh, M.R. Singh, Polymers in topical delivery of anti-psoriatic medications and other topical agents in overcoming the barriers of conventional treatment strategies, *Progress in Biomaterials*. (2021). <https://doi.org/10.1007/s40204-021-00154-7>.
 6. P. Semwal, S. Painuli, T. Abu-Izneid, A. Rauf, A. Sharma, S.D. Daştan, M. Kumar, M.M. Alshehri, Y. Taheri, R. Das, S. Mitra, T. Bin Emran, J. Sharifi-Rad, D. Calina, W.C. Cho, Diosgenin: An Updated Pharmacological Review and Therapeutic Perspectives, *Oxidative Medicine and Cellular Longevity*. (2022). <https://doi.org/10.1155/2022/1035441>.
 7. B. Koul, P. Taak, A. Kumar, A. Kumar, I. Sanyal, Genus Psoralea: A review of the traditional and modern uses, phytochemistry and pharmacology, *Journal of Ethnopharmacology*. (2019). <https://doi.org/10.1016/j.jep.2018.11.036>.
 8. B.H.J. Gowda, M.G. Ahmed, A. Husain, Transfersomal in situ gel administered through umbilical skin tissues for improved systemic bioavailability of drugs: A novel strategy to replace conventional transdermal route, *Medical Hypotheses*. (2022). <https://doi.org/10.1016/j.mehy.2022.110805>.
 9. Mahima ., Kajal Tomer, Dharmendra Kumar, Pramod Kumar Sharma, Preparation and Characterization of a Coconut Oil Nanoemulsion for Ellagic Acid Encapsulation, *Current Nanomaterials*; Volume 11, Issue , Year 2026, e24054615375040. DOI: 10.2174/0124054615375040251003113615
 10. Manish Kumar, Dharmendra Kumar, Formulation and Evaluation of Quercetin Loaded Sago Starch Nanoparticles, *Current Nanomedicine*, Volume 15, Issue 5, 2025, Pages 637-645, <https://doi.org/10.2174/0124681873299675240628125625>.
 11. S.R. Varma, T.O. Sivaprakasam, A. Mishra, S. Prabhu, M. Rafiq, P. Rangesh, Imiquimod-induced psoriasis-like inflammation in differentiated Human keratinocytes: Its evaluation using curcumin, *European Journal of Pharmacology*. (2017). <https://doi.org/10.1016/j.ejphar.2017.07.040>.
 12. V. Bourganis, O. Kammona, A. Alexopoulos, C. Kiparissides, Recent advances in carrier mediated nose-to-brain delivery of pharmaceuticals, *European Journal of Pharmaceutics and Biopharmaceutics*. (2018). <https://doi.org/10.1016/j.ejpb.2018.05.009>.
 13. T.P. Sari, B. Mann, R. Kumar, R.R.B. Singh, R. Sharma, M. Bhardwaj, S. Athira, Preparation and characterization of nanoemulsion encapsulating curcumin, *Food Hydrocolloids*. (2015). <https://doi.org/10.1016/j.foodhyd.2014.07.011>.
 14. M.M. Albahri, A.S.A. Mamri, Z.A. Fawaz, N.S. Lotfi, F. Auf, M. Balamurugan, M.S. Akhtar, Formulation and Evaluation of Shampoo Comprising Polyherbal Extracts, *Journal of Pharmacological Research and Developments*. (2022). <https://doi.org/10.46610/jprd.2022.v04i01.002>.
 15. V. Kumar, S. Ain, B. Kumar, Q. Ain, Gaurav, Optimization and evaluation of topical gel containing solid lipid nanoparticles loaded with luliconazole and its anti-fungal activity, in: *International Journal of Pharmaceutical Research*, 2020: pp. 2901–2912. <https://doi.org/10.31838/ijpr/2020.SP2.169>.
 16. V. Kumar, P. Sharma, L. Chourisia, DEVELOPMENT, CHARACTERIZATION, AND EVALUATION OF TOPICAL GEL FORMULATED WITH LULICONAZOLE-LOADED SOLID LIPID NANOPARTICLES, 15 (2024) 3531–3547. [https://doi.org/10.13040/IJPSR.0975-8232.15\(12\).3531-47](https://doi.org/10.13040/IJPSR.0975-8232.15(12).3531-47).
 17. T.K. Marwaha, K. Bhise, Formulation Development of Anti-psoriatic Topical Babchi Oil Emulgel Anti Psoriatic Emulgel , *Journal of Herbal Science*. (2013).
 18. A. Gull, S. Ahmed, F.J. Ahmad, U. Nagaich, A. Chandra, Hydrogel thickened microemulsion; a local cargo for the co- delivery of cinnamaldehyde and berberine to treat acne vulgaris, *Journal of Drug Delivery Science and Technology*. (2020). <https://doi.org/10.1016/j.jddst.2020.101835>.
 19. A. Ali, S. Ali, M. Aqil, S.S. Imam, A. Ahad, A. Qadir, Thymoquinone loaded dermal lipid nano particles: Box Behnken design optimization to preclinical psoriasis assessment, *Journal of Drug Delivery Science and Technology*. (2019). <https://doi.org/10.1016/j.jddst.2019.05.041>.
 20. Dharmendra Kumar, Pramod Kumar Sharma, Wound Healing, Anti-inflammatory and Antioxidant Potential of Quercetin Loaded Banana Starch Nanoparticles, *Anti-Inflammatory & Anti-Allergy Agents in Medicinal Chemistry*; Volume 22, Issue 4, Year 2023, e261023222769. DOI: 10.2174/0118715230252770231020060606
 21. Dharmendra Kumar, Pramod Kumar Sharma, Formulation and Evaluation of Quercetin-loaded Banana Starch Nanoparticles, *Nanoscience & Nanotechnology-Asia*; Volume 13, Issue 4, Year 2023, e240523217291. DOI: 10.2174/2210681213666230524145559
 22. M. Ferreira, L. Barreiros, M.A. Segundo, T. Torres, M. Selores, S.A. Costa Lima, S. Reis, Topical co-delivery of methotrexate and etanercept using lipid nanoparticles: A targeted approach for psoriasis management, *Colloids and Surfaces B: Biointerfaces*. (2017). <https://doi.org/10.1016/j.colsurfb.2017.07.080>.
 23. A. Jain, V. Pooladanda, U. Bulbake, S. Doppalapudi, T.A. Rafeeqi, C. Godugu, W. Khan, Liposphere mediated topical delivery of

- thymoquinone in the treatment of psoriasis, *Nanomedicine: Nanotechnology, Biology, and Medicine*. (2017). <https://doi.org/10.1016/j.nano.2017.06.009>.
24. P. Sathe, R. Saka, N. Kommineni, K. Raza, W. Khan, Dithranol-loaded nanostructured lipid carrier-based gel ameliorate psoriasis in imiquimod-induced mice psoriatic plaque model, *Drug Development and Industrial Pharmacy*. (2019). <https://doi.org/10.1080/03639045.2019.1576722>.
 25. V.N. Nerella, M. Näther, A. Iqbal, M. Butler, V. Mechtcherine, Inline quantification of extrudability of cementitious materials for digital construction, *Cement and Concrete Composites*. (2019). <https://doi.org/10.1016/j.cemconcomp.2018.09.015>.
 26. S. Sahu, S.S. Katiyar, V. Kushwah, S. Jain, Active natural oil-based nanoemulsion containing tacrolimus for synergistic antipsoriatic efficacy, *Nanomedicine*. (2018). <https://doi.org/10.2217/nmm-2018-0135>.
 27. L. Bhatt, R.D. Kale, Lemongrass (*Cymbopogon Flexuosus* Steud.) was treated textile: A control measure against vector-borne diseases, *Heliyon*. (2019). <https://doi.org/10.1016/j.heliyon.2019.e02842>.
 28. A. Banerjee, J. Binder, R. Salama, J.F. Trant, Synthesis, characterization and stress-testing of a robust quillaja saponin stabilized oil-in-water phytocannabinoid nanoemulsion, *Journal of Cannabis Research*. (2021). <https://doi.org/10.1186/s42238-021-00094-w>.
 29. M. Nasr, Development of an optimized hyaluronic acid-based lipidic nanoemulsion co-encapsulating two polyphenols for nose to brain delivery, *Drug Delivery*. (2016). <https://doi.org/10.3109/10717544.2015.1092619>.
 30. N.H. Arbain, N. Salim, W.T. Wui, M. Basri, M.B.A. Rahman, Optimization of quercetin loaded palm oil ester based nanoemulsion formulation for pulmonary delivery, *Journal of Oleo Science*. (2018). <https://doi.org/10.5650/jos.ess17253>.
 31. N.A. Wahgiman, N. Salim, M.B.A. Rahman, S.E. Ashari, Optimization of nanoemulsion containing gemcitabine and evaluation of its cytotoxicity towards human fetal lung fibroblast (MRC5) and human lung carcinoma (A549) cells, *International Journal of Nanomedicine*. (2019). <https://doi.org/10.2147/IJN.S212635>.
 32. Chanchal Tiwari, Arjun Singh, Dharmendra Kumar, Comprehensive Characterization and In vitro Evaluation of a Novel POQCL Drug Delivery System, *Nanoscience & Nanotechnology-Asia*; Volume 13, Issue 6, Year 2023, e071223224207. DOI: 10.2174/0122106812276945231201071629
 33. Manish Kumar, Dharmendra Kumar, Formulation and Evaluation of Quercetin Loaded Sago Starch Nanoparticles, *Current Nanomedicine*; Volume 15, Issue 5, Year 2025, e230724232199. DOI: 10.2174/0124681873299675240628125625
 34. V.K. Kumar, R.R. Devi, E. Hemanathan, In vitro studies to analyze the stability and bioavailability of thymoquinone encapsulated in the developed nanocarrier, *Journal of Dispersion Science and Technology*. (2020). <https://doi.org/10.1080/01932691.2018.1564672>.
 35. H. Kausar, M. Mujeeb, A. Ahad, T. Moolakkadath, M. Aqil, A. Ahmad, M.H. Akhter, Optimization of ethosomes for topical thymoquinone delivery for the treatment of skin acne, *Journal of Drug Delivery Science and Technology*. (2019). <https://doi.org/10.1016/j.jddst.2018.11.016>.
 36. H. Demirel, C. Arlı, T. Özgür, M. İnci, R. Dokuyucu, The role of topical thymoquinone in the treatment of acute otitis externa; an experimental study in rats, *Journal of International Advanced Otolaryngology*. (2018). <https://doi.org/10.5152/iao.2017.4213>.
 37. A. Singh, I. Ahmad, S. Akhter, G.K. Jain, Z. Iqbal, S. Talegaonkar, F.J. Ahmad, Nanocarrier based formulation of Thymoquinone improves oral delivery: Stability assessment, in vitro and in vivo studies, *Colloids and Surfaces B: Biointerfaces*. (2013). <https://doi.org/10.1016/j.colsurfb.2012.08.038>.
 38. F.O. Alotaibi, G. Mustafa, A. Ahuja, STUDY OF ENHANCED ANTI-INFLAMMATORY POTENTIAL OF NIGELLA SATIVA IN TOPICAL NANOFORMULATION, *International Journal of Pharmacy and Pharmaceutical Sciences*. (2018). <https://doi.org/10.22159/ijpps.2018v10i7.22966>.
 39. R. Abu-Dahab, F. Odeh, S.I. Ismail, H. Azzam, A. Al Bawab, Preparation, characterization and antiproliferative activity of thymoquinone- β -cyclodextrin self assembling nanoparticles, *Pharmazie*. (2013). <https://doi.org/10.1691/ph.2013.3033>.
 40. C.T. Selçuk, M. Durgun, R. Tekin, L. Yolbas, M. Bozkurt, C. Akçay, U. Alabalk, M.K. Basarali, Evaluation of the Effect of Thymoquinone Treatment on Wound Healing in a Rat Burn Model, *Journal of Burn Care and Research*. (2013). <https://doi.org/10.1097/BCR.0b013e31827a2be1>.
 41. M. Elmowafy, A. Samy, M.A. Raslan, A. Salama, R.A. Said, A.E. Abdelaziz, W. El-Eraky, S. El Awdan, T. Viitala, Enhancement of Bioavailability and Pharmacodynamic Effects of Thymoquinone Via Nanostructured Lipid Carrier (NLC) Formulation, *AAPS PharmSciTech*. (2016). <https://doi.org/10.1208/s12249-015-0391-0>.
 42. Dharmendra Kumar, Rishabha Malviya, Pramod K. Sharma, Akanksha Sharma, Vineet Bhardwaj, Advancement in Nano Pharmaceutical Formulations and their Biomedical Use, *Nanoscience & Nanotechnology-Asia*; Volume 11, Issue 3, Year 2021, DOI: 10.2174/2210681210999200723165456
 43. K. Gnananath, K.S. Nataraj, B.G. Rao, K.P. Kumar, K. Chandrasekhar, P. Jain, M.A. Mirza, Ternary

- System of Bacogenins with Fulvic Acid and Hydrogenated Soy Lecithin: Preparation, Characterization and, In vivo Studies, Current Topics in Medicinal Chemistry. (2021). <https://doi.org/10.2174/15680266216662111111554> 25.
44. S.P. Agarwal, M.K. Anwer, M. Aqil, Complexation of furosemide with fulvic acid extracted from shilajit: A novel approach, Drug Development and Industrial Pharmacy. (2008). <https://doi.org/10.1080/03639040701744053>.
45. C. Huang, P. Hu, Q. Wu, M. Xia, W. Zhang, Z. Lei, D.-X. Li, G. Zhang, J. Feng, Preparation, in vitro and in vivo Evaluation of Thermosensitive in situ Gel Loaded with Ibuprofen-Solid Lipid Nanoparticles for Rectal Delivery, Drug Design, Development and Therapy. Volume 16 (2022) 1407–1431. <https://doi.org/10.2147/DDDT.S350886>.
46. M. Kamran, A. Ahad, M. Aqil, S.S. Imam, Y. Sultana, A. Ali, Design, formulation and optimization of novel soft nano-carriers for transdermal olmesartanmedoxomil delivery: In vitro characterization and in vivo pharmacokinetic assessment, International Journal of Pharmaceutics. (2016). <https://doi.org/10.1016/j.ijpharm.2016.03.030>.
47. Chanchal Tiwari, Jigyasa Tomer, Dharmendra Kumar, Liposomal Drug Delivery: Progress, Clinical Outlook, and Ongoing Challenges, Recent Advances in Drug Delivery and Formulation; Volume 18, Issue 3, Year 2024, e090724231741. DOI: 10.2174/0126673878300031240703070511
48. S. Kumar, J. Ali, S. Baboota, Design Expert® supported optimization and predictive analysis of selegiline nanoemulsion via the olfactory region with enhanced behavioural performance in Parkinson's disease, Nanotechnology. (2016). <https://doi.org/10.1088/0957-4484/27/43/435101>.